Since January 2020 Elsevier has created a COVID-19 resource centre with free information in English and Mandarin on the novel coronavirus COVID-19. The COVID-19 resource centre is hosted on Elsevier Connect, the company's public news and information website.

VIROLOGY 209, 337–346 (1995)

Evolution of Mouse Hepatitis Virus (MHV) during Chronic Infection: Quasispecies Nature of the Persisting MHV RNA

CECILIA ADAMI,* JOAN POOLEY,† JULIET GLOMB,* ERIC STECKER,† FABEHA FAZAL,* JOHN O. FLEMING,† and SUSAN C. BAKER*,[1]

*Department of Microbiology and Immunology, Loyola University of Chicago Stritch School of Medicine, Maywood, Illinois 60153; and †Departments of Neurology and Medical Microbiology, University of Wisconsin and William S. Middleton Veterans Hospital, Madison, Wisconsin 53792

Received December 24, 1994; accepted March 14, 1995

Coronavirus infection of mice has been used extensively as a model for the study of acute encephalitis and chronic demyelination. To examine the evolution of coronavirus RNA during chronic demyelinating infection, we isolated RNA from intracerebrally inoculated mice at 4, 6, 8, 13, 20, and 42 days postinfection and used reverse transcription–polymerase chain reaction amplification methods (RT–PCR) to detect viral sequences. RNA sequences from two viral structural genes, the spike gene and the nucleocapsid gene, were detected throughout the chronic infection. In contrast, infectious virus was not detectable from brain homongenates beyond 13 days postinfection. These results indicate that coronavirus RNA persists in the brain at times when infectious virus is not detected. To determine if genetic changes were occurring during viral replication in the host, we cloned and sequenced the RT–PCR products from the spike and nucleocapsid regions and analyzed the sequences for mutations. Sequencing of the cloned products revealed that a variety of mutant forms of viral RNA persisted in the CNS, including point mutants, deletion mutants, and termination mutants. The mutations accumulated during persistent infection in both the spike and the nucleocapsid sequences, with greater than 65% of the mutations encoding amino acid changes. These results show that a diverse population or quasispecies consisting of mutant and deletion variant viral RNAs (which may not be capable of producing infectious virus particles) persists in the central nervous system of mice during chronic demyelinating infection. The implications of these results for the role of persistent viral genetic information in the pathogenesis of chronic demyelination are discussed.

INTRODUCTION

Mouse hepatitis virus (MHV) is an enveloped virus with a 31-kb single-stranded RNA genome (Lai, 1990; Spaan *et al.*, 1990). The virion particle is composed of three glycoproteins (S, spike; M, matrix; and HE, hemagglutinin-esterase) and the nucleocapsid protein (N), which is associated with the MHV RNA. MHV replicates in the cytoplasm of infected cells using a viral RNA-dependent RNA polymerase that is translated from the genomic RNA. In infected rodents, MHV is able to replicate in the central nervous system (CNS), resulting in acute encephalitis and chronic demyelination. Infection of rodents with strains of MHV which induce predominantly chronic demyelination has been used as a model system for studying human demyelinating diseases such as multiple sclerosis.

Many laboratories have used the MHV model system to investigate the role of the virus and the immune system in chronic demyelination. These studies have shown that viral structural genes such as the spike and hemagglutinin-esterase are important in determining the neuropathogenicity (encephalitis versus chronic demyelination) of the virus and in the ability of the virus to spread through the CNS (reviewed by Kyuwa and Stohlman, 1990). However, it has been difficult to assess the role of the virus in chronic infection because infectious virus is rarely isolated after 20 days postinfection (Knobler *et al.*, 1982; Dalziel *et al.*, 1986; Yokomori *et al.*, 1993) and may not be representative of the persistent viral RNA population. Therefore, we elected to analyze the evolution of MHV RNA by examining specific regions of the RNA throughout the chronic infection. The specific regions examined were the S1 portion of the spike glycoprotein gene and a portion of the nucleocapsid gene. These regions were selected because they encode viral structural proteins important in the pathogenesis of the disease. The S1 region of the spike glycoprotein has previously been characterized as "hypervariable" (Banner *et al.*, 1990), whereas the nucleocapsid region is more conserved among MHV strains.

In this study, we report the evolution of coronavirus RNA during persistent infection. We infected mice with a strain of MHV which consistently caused demyelination (Fleming *et al.*, 1986) and analyzed the viral RNA isolated from the brain at various time points after infection. The viral RNA was detected by reverse transcription–polymerase chain reaction amplification methodology. By se-

[1] To whom correspondence should be addressed.

0042-6822/95 $6.00

quence analysis of the amplified products, we found that MHV RNA persists in the brains of infected animals in multiple mutant/defective forms. The majority of the mutations we detected were biased transitions (U to C and A to G) and resulted in amino acid changes. These results demonstrate the rapid evolution of coronavirus RNA during persistent infection and suggest that a diverse population of coronavirus RNA persists in the central nervous system where it may contribute to the pathogenesis of chronic demyelination.

MATERIALS AND METHODS

Virus

MHV-JHM antigenic variant 2.2-V-1 was propagated in DBT cells and quantitated by plaque assay as previously described (Fleming *et al.,* 1986). This low virulence variant was selected by resistance to neutralization by an antibody directed against the spike glycoprotein (Fleming *et al.,* 1986) and causes predominantly chronic demyelination in mice (Fleming *et al.,* 1986). Relative to the parental virus, JHM-DL, from which it was selected, MHV-JHM 2.2-V-1 encodes a single nucleotide change in the S2 region of the spike gene (nucleotide 3340) which results in an amino acid change from leucine to phenylalanine (Wang *et al.,* 1992).

Animal experiments

Six-week-old male C57BL/6J mice (Jackson Laboratories, Bar Harbor, ME) were used in all experiments. Upon arrival, selected mice were screened by enzyme-linked immunosorbent assay (Fleming and Pen, 1988) and found to be seronegative for murine coronaviruses. Mice were inoculated intracerebrally with 10^3 plaque forming units (PFU) of MHV-JHM 2.2-V-1 diluted in 30 μl Dulbecco's modified minimal essential medium. At the indicated times, mice were sacrificed by CO_2 inhalation, and brains were removed aseptically, immediately frozen on dry ice, and stored at −70°. In representative animals, viral titers were determined on one-half of the fresh, unfrozen brain by plaque assay as previously described (Fleming *et al.,* 1986).

RNA extraction

Brains were thawed, and each half brain was manually disrupted in a Tenbrock homogenizer containing 2 ml phenol/chloroform (1/1) and 2 ml of lysis buffer (0.5% SDS, 0.025 *M* EDTA, 0.074 *M* NaCl). RNA was subsequently extracted once with lysis buffer, and proteins removed by extraction with phenol/chloroform (1/1) and with chloroform. RNA was precipitated first in the presence of 3.0 *M* ammonium acetate (final concentration) and incubated overnight at −20°. The RNA was pelleted by centrifugation for 15 min at 10,000 *g* and the pellet was resuspended in DEPC-treated water. The RNA was reprecipitated in the presence of 0.3 *M* sodium acetate and 2.5 volumes of ethanol. RNA from four to six brains were combined in order to prepare representative pools from each time point. RNA quantity was determined by optical density measurements at 260 nm.

Input virus RNA was isolated by mixing 5×10^6 PFU of MHV-JHM 2.2-V-1 with one-half of an uninfected mouse brain and immediately subjecting the mixture to RNA extraction as described above.

Reverse transcription–polymerase chain reaction (RT–PCR) of brain RNA

Two micrograms of total brain RNA was denatured with 20 m*M* methylmercury hydroxide for 5 min at room temperature, after which β-mercaptoethanol was added at a final concentration of 0.14 *M*. For cDNA synthesis, the RNA was incubated at 42° for 60 min in a reaction containing 50 m*M* Tris–HCl (pH 8.3), 50 m*M* KCl, 10 m*M* $MgCl_2$, 10 m*M* DTT, 0.5 m*M* spermidine, 1.25 m*M* of each dNTP, 40 units RNasin, 1 μg random hexamer oligonucleotide primers, and 4 units avian myeloblastosis virus reverse transcriptase (Promega, Madison, WI). The mixture was incubated at 95° for 3 min, cooled on ice for 1 min, and incubated at 42° for 60 min after the addition of another 4 units of reverse transcriptase.

The synthesized cDNA was amplified by PCR using a method adapted from Saiki *et al.* (1988) and Chang *et al.* (1993) to minimize *Taq* errors. Briefly, 20 μl of reverse transcription mixture was mixed with 80 μl of a master mix buffer containing 7.5 m*M* Tris–Cl (pH 9.0), 37.5 m*M* KCl, 0.075% Triton X-100, 0.84 m*M* $MgCl_2$, 0.25 μ*M* synthetic oligonucleotide primers, and 2.5 units of *Taq* polymerase (Promega). The reaction mixture was overlaid with 50 μl mineral oil and subjected to 30 (Fig. 2B) or 35 (Fig. 2A) cycles of amplification with each cycle consisting of 94° for 1 min, 60° for 1 min, and 72° for 1 min. At the end of this period, an additional extension step at 72° for 7 min was performed. MHV-JHM nucleotide sequences for oligonucleotide PCR primers are indicated in Table 1. RT–PCR products were resolved by electrophoresis on a 1.2% agarose gel in 1× TAE buffer (0.04 *M* Tris–acetate, pH 8.5, 0.002 *M* EDTA) and stained with ethidium bromide.

cDNA cloning and sequencing

PCR-amplified products generated by 35 cycles of amplification of the S1 and N genes were purified using the Magic PCR Preps DNA purification system (Promega) and ligated into the pGEM-T vector (Promega). The ligation buffer contained 30 m*M* Tris–Cl, pH 7.8, 10 m*M* $MgCl_2$, 10 m*M* DTT, and 0.5 m*M* ATP and 3 units of T4 DNA ligase. The ligation product was used to transform competent *Escherichia coli* strain DH5α (BRL). Plasmid DNA was isolated from the bacteria by Magic Miniprep purification resin (Promega) and sequenced by the

TABLE 1

Oligonucleotide Primers Used to Amplify MHV Sequences

Primer	Sequence (5′ to 3′)[a]	Position[b]
SI-1	TATGAATTCTACGTTATGTCCAGGCTGAGTC	1084–1106
SI-2	TATGGATCCATAGAGGTCATATCTGACGC	1895–1916
SI-3	ATGTTGCCTACGCCCAGC	1391–1408
SI-4	CACTCACGATGAATTGTGCC	1510–1529
AM8-1	CCAAGCTTCTGCACCTGCTAGTCGATCTG	672–693
AM8-2	CCGGTACCACCATCTTGATTCTGGTAGGC	1215–1237
AM8-3	ATGAATTCAGCGCAAGCCTGCCTCTACTG	747–768
AM8-4	ATGGATCCTGAATATTGCAGCTCATACAC	1122–1144

[a] Additional nucleotides (underlined) provide restriction endonuclease recognition sites.

[b] Nucleotide position of SI according to Parker *et al.* (1989). Nucleotide position of N according to Skinner *et al.* (1983).

Sanger dideoxy chain termination method (Sanger *et al.*, 1977) using Sequenase Enzyme 2.0 (Sequenase DNA sequencing kit, version 2.0, U.S. Biochemicals) with reverse and −40 primers. Internal primers for the spike 1 region and nucleocapsid region (SI-3, SI-4, AM8-3, and AM8-4, see Table 1) were used in some sequencing reactions. Reaction products were analyzed on 5% Hydrolink (J. T. Baker) gels containing 7 *M* urea in TBE.

RESULTS

Persistence of MHV-JHM RNA

To examine the evolution of coronavirus RNA during chronic demyelinating infection, we extracted brains from mice at 4, 6, 8, 13, 20, and 42 days postinfection and analyzed them for infectious virus and viral RNA. We were able to detect production of infectious virus until 13 days post infection (data not shown) by plaque assay of brain homogenates. To determine whether coronavirus RNA persists in mouse brains beyond times when infectious virus is detected, we performed RT–PCR using primers specific to the S1 region of the spike glycoprotein and to the nucleocapsid gene (Fig. 1). We were able to amplify both the spike (Fig. 2A) and the nucleocapsid (Fig. 2B) sequences from total RNA isolated from MHV-infected mouse brain at 4, 6, 8, 13, 20, and 42 days. PCR products of the expected 832-bp size for the S1 region and of the 565-bp size for the nucleocapsid region were detected. No PCR product was detected in the reagents alone control (Figs. 2A and 2B, lane C) or uninfected brain RNA (Figs. 2A and B, lane U). As shown in Figs. 2A and 2B, the RT-PCR products of the S1 and the nucleocapsid genes were detected at 42 days postinfection without resorting to additional cycles of amplification or the use of nested primers. Clearly the amount of viral RNA decreases significantly after 13 days postinfection; however, these results demonstrate that coronavirus RNA persists in the brains of infected mice as long as 42 days postinfection. Indeed, preliminary results suggest that coronavirus RNA may persist in the brain of infected mice for the life of the animal (Pooley and Fleming, unpublished).

Sequencing of viral cDNA PCR products

To confirm the identity of the PCR products and to examine the evolution of viral RNAs during chronic infection, we cloned and sequenced the S1 and nucleocapsid PCR products from brain samples taken at 4, 8, 13, 20, and 42 days p.i. To control for mutations generated during the RNA isolation and RT–PCR amplification process, we mixed input virus particles (5×10^6 PFU) with uninfected brain and immediately subjected the mixture to RNA extraction and RT–PCR amplification (see Materials and Methods). The PCR products were ligated into the plasmid pGEM-T as described under Materials and Methods and individual clones were sequenced by the Sanger dideoxy chain termination method (Sanger *et al.*, 1977). The mutations detected in each clone are listed in Table 2 and summarized in Table 3. Sequencing of eight clones representing input virus showed that seven of the eight clones encoded the wild-type sequence. A single mutation (A to G) was detected in one clone (S0-8). These results reflect the "master" sequence (wild type) typically found in the virus population derived from tissue culture cells (Steinhauer and Holland, 1987). In contrast, sequencing of individual clones at 4, 8, 13, 20, and 42 days postinfection showed that multiple point mutants and deletion mutants are detectable in the persistent RNA population (Table 3). These results are consistent with an increase in the diversity of the quasispecies in the persistent MHV RNA population.

A total of 20 individual clones were sequenced from PCR products generated at Day 4 postinfection. There was an average of 1 mutation per clone, with 5 of the 20 clones containing wild-type sequences. In the samples generated from RNA isolated at 42 days postinfection, we detected an increase in the number of mutations (55 mutations in 20 clones), with only 1 of 20 clones encoding wild-type sequence. The mutations were spread throughout the S1 region (Fig. 3). There was an average of 2 to 3 mutations per clone (range 0 to 6) and 1 clone contained a deletion from nucleotides 1529 to 1618. The same deletion was detected in a Day 8 clone, suggesting that this deletion variant may be generated early during the course of infection. It is striking that this particular deletion mutant is present in independently isolated brain RNA samples (Day 8 and Day 42). Interestingly, several

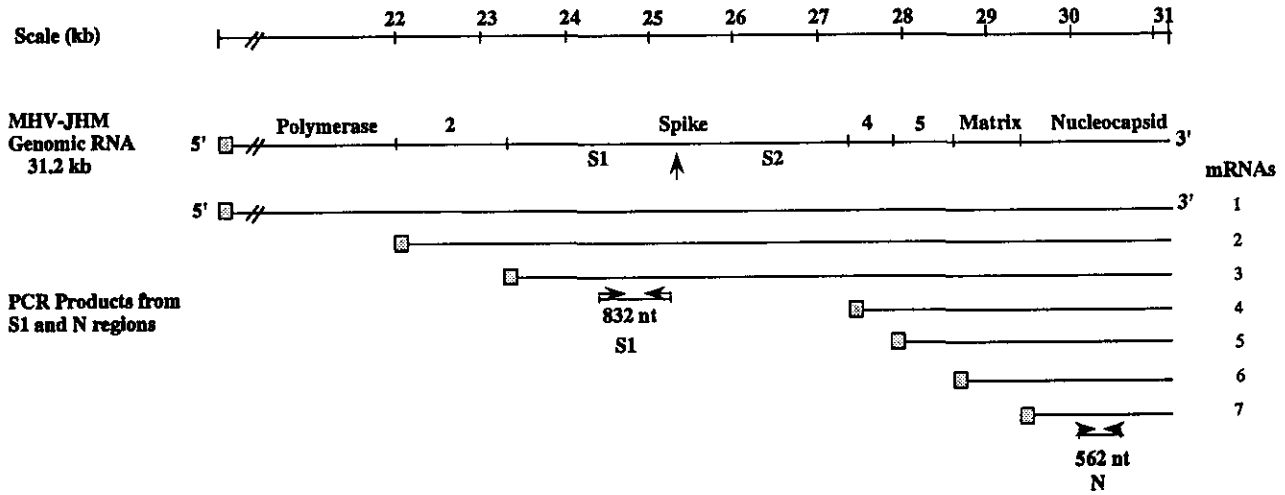

FIG. 1. Schematic representation of the 31-kb MHV-JHM genome and seven mRNAs. The shaded boxes represent the viral leader sequences that are at the 5'-end of each of the mRNAs. The 22-kb polymerase gene is not drawn to scale. Arrows exemplify the primers used to amplify specific regions of spike and nucleocapsid sequences.

other attenuated variants have been described in which this region of the S1 has been deleted (Dalziel *et al.*, 1986; Fleming *et al.*, 1986; Morris *et al.*, 1989; Parker *et al.*, 1989; La Monica *et al.*, 1991; Wang *et al.*, 1992). This region (from nt 1500 to nt 1959) has in fact been termed "hypervariable" (Banner *et al.*, 1990; Wang *et al.*, 1992). However, the mutations we detected were not limited to the hypervariable region, but were distributed throughout the S1 region (Fig. 3).

To further investigate the evolution of the MHV RNA, we examined a second region of the virus, the nucleocapsid region. The sequence analysis of the nucleocapsid PCR products revealed a pattern similar to that seen in the S1 gene, that is, an increased number of mutations in the persistent RNA (Tables 4 and 5). At Day 4 post infection, 11 of 20 clones maintained the wild-type sequence and the remaining clones encoded one or two mutations per clone. In contrast, only 8 of the 20 clones randomly isolated at 42 days post infection maintained the wild-type nucleic acid sequence. These results indicate that mutations may potentially occur throughout the RNA genome.

To determine whether there was a bias for any type of mutations during persistent infection, we categorized the mutations as transitions or transversions (Table 6). Analysis of the type of the nucleotide changes detected during coronavirus persistent infection revealed that the mutations consisted predominantly of U to C and A to G transitions (Table 6, 85 U to C and A to G mutations/135 total mutations; 63%). Biased mutations, most dramatically seen in persistent measles infection (Cattaneo *et al.*, 1988), have been proposed to occur due to modification of double stranded RNA intermediates that form during viral RNA transcription and replication by the cellular helicase activity (Bass *et al.*, 1989, see Discussion). Overall, the persisting MHV RNA contains a variety of mutations, the majority (65%) of which encode amino acid

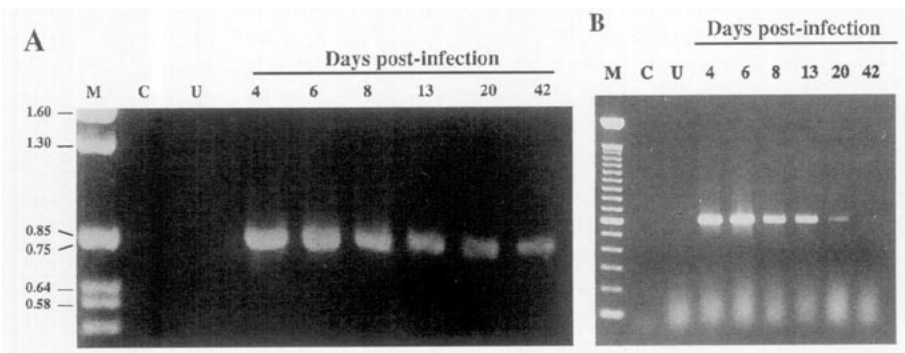

FIG. 2. *Long-term persistence of MHV-JHM 2.2-V-1 RNA in brains of C57/B16 mice. Brain RNA was isolated at 4, 6, 8, 13, 20, and 42 days* postinoculation and subjected to RT–PCR amplification of 35 cycles using spike-specific primers (A) and 30 cycles using nucleocapsid-specific primers (B). Lane C shows no products were amplified from reagents alone; lane U shows no products were amplified from uninfected brain RNA. Lane M indicates DNA standards (A) and 100 bp marker DNA (B). Products were analyzed by electrophoresis on a 1.2% agarose gel and visualized by staining with ethidium bromide.

TABLE 2

Mutations Detected in the Spike S1 Region during Persistent MHV-JHM Infection

Clone	Nucleotide	Codon change	Amino acid
Day 0: 8 clones sequenced, 7 clones encoded wild type sequence			
S0-8	1127 A → G	GAU → GGU	Asp → Gly
Day 4: 20 clones sequenced, 5 clones encoded wild-type sequence			
S4-1	1335 U → C	UCU → UCC	No change
	1878 A → G	GAA → GAG	No change
S4-4	1783 G → C	GUA → CUA	*Val* → *Leu*
	1734 U → C	UGU → UGC	No change
S4-5	1118 A → G	AAU → AGU	Asn → Ser
S4-7	1741 G → A	GCC → ACC	Ala → Thr
S4-8	1767 A → G	UCA → UCG	No change
S4-9	1667 G → A	GGC → GAC	Gly → Asp
S4-10	1205 A → G	GAU → GGC	Asp → Gly
	1675 U → C	UGU → CGU	Cys → Arg
S4-11	1167 A → G	UCA → UCG	No change
	1841 C → U	ACU → AUU	Thr → Ile
S4-12	1299 G → A	AAG → AAA	No change
	1509 A → G	ACA → ACG	No change
S4-14	1230 U → C	UUU → UUC	No change
S4-16	1560 G → A	UCG → UCA	No change
	1797 C → U	UGC → UGU	No change
S4-17	1336 U → C	UGG → CGG	Trp → Arg
	1869 U → C	CCU → CCC	No change
S4-18	1261 G → C	GCU → CCU	Ala → Pro
S4-19	1232 U → C	UUG → UCG	Leu → Ser
S4-20	1869 U → C	CCU → CCC	No change
Day 8: 4 clones sequenced			
S8-2	1432 U → C	UAU → CAU	Tyr → His
S8-3	1697 A → G	GAA → GGA	Glu → Gly
S8-4	1529-1618	DELETION	
S8-6	1233 G → A	UUG → UUA	No change
	1332 G → A	UCG → UCA	No change
Day 13: 4 clones sequenced			
S13-1	1349 U → C	UAU → CAU	Try → His
	1468 U → C	UGC → CGC	Cys → Arg
S13-4	1288 U → C	CUU → CUC	No change
	1592 A → G	GAG → GGG	Glu → Gly
	1760 G → A	GGA → GAA	Gly → Glu
S13-5	1285 U → C	AGU → AGC	No change
	1595 G → A	UGC → UAC	Cys → Try
	1763 G → A	UGG → UAG	Trp → TERM
S13-6	1543 G → U	GGG → UGG	Gly → Trp
	1726 A → U	AAG → UAG	Lys → TERM
Day 20: 4 clones sequenced			
S20-5	1394 U → C	GUU → GCU	Val → Gly
	1367 G → A	GGU → GAU	Gly → Asp
S20-6	1192 A → G	AGC → GGC	Ser → Gly
	1413 U → C	UGU → UGC	No change
S20-7	1289 U → C	AGU → AGC	No change
	1628 A → G	GAU → GGU	Asp → Gly
S20-8	1109 U → C	UUU → UUC	No change
Day 42: 20 clones sequenced, 1 clone encoded wild-type sequence			
S42-2	1416 U → C	UUU → UUC	No change
	1472 C → U	ACU → AUU	Thr → Ile
	1546 C → U	CCC → UCC	Pro → Ser
S42-3	1271 C → U	UCA → UUA	Ser → Leu
	1480 A → G	ACC → GCC	Thr → Ala
S42-1	1688 G → A	GGU → GAU	*Gly* → *Asp*
	1764 G → A	UGG → UGA	Trp → TERM
S42-7	1266 C → U	GCC → GCU	No change
	1280 U → C	CUG → CCG	Leu → Pro
	1313 A → G	AUA → GUA	Ile → Asp
	1518 U → C	AUU → AUC	No change
	1800 A → U	CAA → CAU	Gln → His
S42-13	1215 U → A	AUU → AUA	No change
	1821 A → G	UUA → UUG	No change
S42-9	1119 U → C	AAU → AAC	No change
	1199 A → G	CAA → CGA	Gln → Arg
S42-12	1173 U → A	GAU → GAA	Asp → Glu
	1529-1618	Deletion	
	1649 A → G	AAA → AGA	Lys → Arg
	1737 U → C	UCU → UCC	No change
	1872 U → C	AAU → AAC	No change
S42-15	1446 A → G	GCA → GCG	No change
	1592 A → G	GAG → GGG	No change
S42-16	1197 U → C	CGU → CGC	No change
	1277 A → G	CAG → CGG	Gln → Arg
	1472 C → U	ACU → AUU	Thr → Ile
	1592 A → G	GAG → GGG	Glu → Gly
	1781 U → C	UUA → UCA	Leu → Ser
S42-17	1090 U → C	UAU → CAU	Tyr → His
	1148 U → A	AUG → AAG	Met → Lys
	1167 A → G	UCA → UCG	No change
S42-18	1212 A → G	CAA → CAG	No change
	1339 A → U	AAU → UAU	Asn → Tyr
	1890 C → G	GGC → GGG	No change
S42-19	1159 A → U	AGU → UGU	Ser → Cys
	1263 U → C	GUU → GCU	Val → Ala
	1764 G → A	UGG → UGA	Trp → TERM
S42-20	1167 A → G	UCA → UCG	No change
	1169 U → C	GUU → GCU	Val → Ala
	1172 A → G	GAU → GGU	Asp → Gly
	1177 U → C	UUU → CUU	Phe → Leu
	1616 U → C	UUU → UCU	Phe → Ser
	1875 U → C	ACU → ACC	No change
S42-21	1870 A → G	AAU → GAU	Asn → Asp
S42-22	1109 U → C	UUG → UCG	Leu → Ser
	1127 A → G	GAU → GGU	Asp → Gly
	1841 C → A	ACU → AAU	Thr → Asn
S42-23	1755 U → C	UCU → CCU	Ser → Pro
S42-24	1156 G → A	GGU → AGU	Gly → Ser
	1311 C → U	ACC → AUC	Thr → Ile
	1631 U → G	CUC → CGC	Leu → Arg
S42-24	1682 G → A	GGU → GAU	Gly → Asp
S42-25	1307 U → C	GUU → GCU	Val → Ala
	1640 G → A	GGG → GAG	Gly → Glu
	1127 A → G	GAU → GGU	Asp → Gly

TABLE 3

Summary of Mutations Detected in the Spike Region during Persistent MHV-JHM Infection

Days postinfection	Clones sequenced	Total mutations detected	Type of mutation[a]				Mutations per thousand nucleotides sequenced
			S	C	Del	Term	
0 (input)	8	1	0	1	0	0	0.2
4	20	22	12	10	0	0	1.4
8	4	5	2	2	1	0	1.7
13	4	10	2	6	0	2	3.4
20	4	7	3	4	0	0	2.4
42	20	55	15	37	1	2	3.7

[a] S, silent; C, change of amino acid; Del, deletion; Term, termination codon.

changes. The diversity of the quasispecies in coronavirus persistent infection may have important implications for chronic pathogenicity.

DISCUSSION

In this study, we examined the evolution of coronavirus RNA during persistent infection. We found that a variety of mutant/defective viral RNAs emerge throughout chronic viral infection in mouse brain and that mutant viral RNAs persist in the brain at times when infectious virus is not detected (after 13 days postinfection). These findings emphasize the diversity and rapid evolution of coronavirus RNA. As early as 8 days postinfection, multiple mutants and a deletion variant were detected. The mutations in the viral RNA were detected in two regions that were examined, the spike S1 and the nucleocapsid region. By 42 days postinfection, the majority of the clones we sequenced contained multiple mutations and/or deletions. Previous studies of chronic MHV infection have shown that infectious viruses with deletions or mutations in the spike gene (Dalziel *et al.*, 1986; Fleming *et al.*, 1986; Morris *et al.*, 1989; Parker *et al.*, 1989; La Monica *et al.*, 1991; Wang *et al.*, 1992) and/or hemagglutinin-esterase gene (Yokomori *et al.*, 1993) can be isolated. In this study, we demonstrate that a mutant or defective viral RNA population, which may not be capable of producing infectious virus, persists in the brain. This defective viral RNA population could potentially contribute to the pathogenesis of chronic demyelination by perturbing normal cell functions and/or by chronically stimulating the immune system (Oldstone, 1989, 1991).

An increase in the heterogeneity in the MHV sequences isolated during the chronic infection is clear for both the spike S1 and the nucleocapsid regions of MHV RNA (Tables 3 and 5). The frequency of mutations we detected in the spike region rose from 1.4 mutations per thousand nucleotides sequenced at Day 4 to 3.7 mutations per thousand nucleotides sequenced at Day 42 (Table 3). The sequencing of individual cDNA clones representing persistent viral RNAs was essential for this study. As shown in Fig. 3, an average of 9 of 10 clones contained the wild-type sequences at any given position. Therefore, sequencing of uncloned PCR products would have revealed an overall wild-type or consensus sequence. By sequencing cloned PCR products, we unveiled a previously undetected diversity in the persistent viral RNA population. This diversity or heterogeneity in the persistent MHV infection is consistent with what has been seen in other persisting RNA viral infections such as measles virus (Baczko, *et al.*, 1986; Cattaneo, *et al.*, 1988), hepatitis delta virus (HDV) (Chao *et al.*, 1990; Lee *et al.*, 1992), and hepatitis C virus (HCV) (Martell *et al.*, 1992; Higashi *et al.*, 1993). In the case of HDV, rapid evolution and microheterogeneity of the viral RNA were demonstrated by isolating, cloning, and sequencing HDV RNA from the serum of a single patient over a 2-year period of chronic infection (Lee *et al.*, 1992). The heterogeneity of HCV has been well documented both in individual patients and in isolates from different geographical regions (Choo *et al.*, 1991; Martell *et al.*, 1992; Higashi *et al.*, 1993). These observations of diversity in persisting RNA virus populations are consistent with the models developed to describe the rapid evolution of RNA viruses and the existence of RNA quasispecies (Steinhauer and Holland, 1987; Eigen, 1993). The evolution of quasispecies in RNA virus infections appears to be a common theme in the development of "smoldering" and chronic viral infections (Martell *et al.*, 1992).

Analysis of the mutations detected in the persistent coronavirus sequences revealed several interesting features. First, the majority of mutations detected in the persistent viral sequences are predicted to encode amino acid changes (65%). The prevalence of mutations that result predominantly in amino acid changes during coronavirus persistence suggests that MHV RNA evolution may be driven by positive selection. One of the most

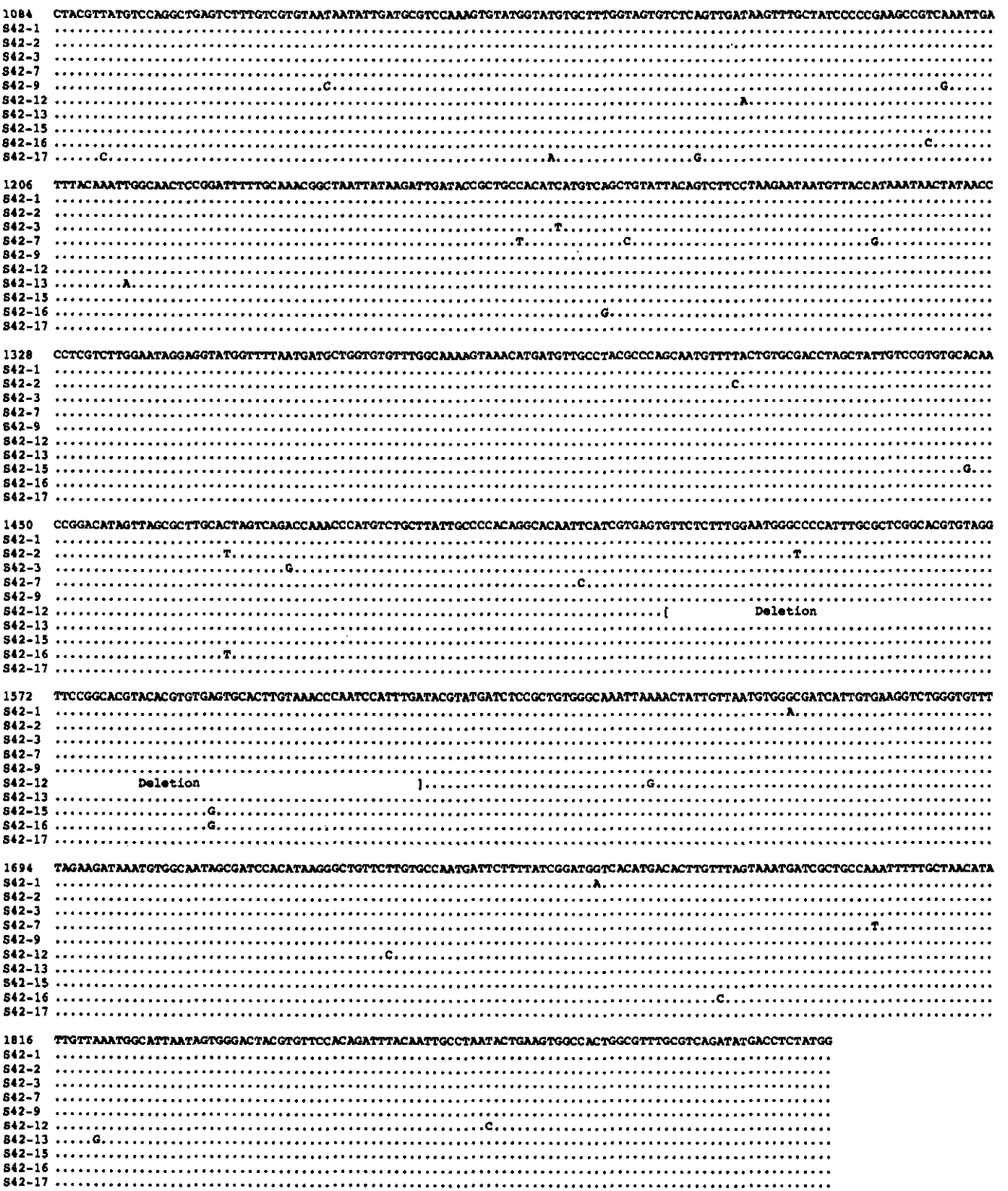

FIG. 3. Multiple mutations detected in the S1 region amplification products synthesized from RNA isolated from mice 42 days after inoculation with MHV-JHM. PCR products were cloned into plasmid pGEM-T and sequenced as described under Materials and Methods. Mutations detected in 10 individual clones are indicated.

TABLE 4

Mutations Detected in the Nucleocapsid Region during Persistent MHV-JHM Infection

Clone	Nucleotide	Codon change	Amino Acid
Day 4: 20 Clones sequenced, 11 clones encoded wild-type sequence			
N4-1	916 A → C	AAC → ACC	Asn → Thr
N4-3	1004 U → C	AGU → AGC	No change
N4-5	857 A → G	CAA → CAG	No change
	1135 A → U	CAA → CUA	Gln → Leu
N4-6	1103 U → C	GCU → GCC	No change
N4-11	956 C → U	GGC → GGU	No change
N4-13	1005 G → A	GAU → AAU	Asp → Asn
N4-20	696 U → C	UCG → CCG	Ser → Pro
N4-25	849 A → G	ACA → GCA	Thr → Ala
N4-29	840 A → G	AAG → GAG	Lys → Glu
	977 C → U	GGC → GGU	No change
Day 20: 4 Clones sequenced, 2 clones encoded wild-type sequence			
N20-6	1087 A → G	AAG → AGG	Lys → Arg
	1163 U → A	AGU → AGA	Ser → Arg
N20-7	990 A → G	AAA → GAA	Lys → Glu
	767 U → C	ACU → ACC	No change
Day 42: 20 Clones sequenced, 8 clones encoded wild-type sequence			
N42-1	1166 U → C	ACU → ACC	No change
N42-2	1116 A → U	AAA → UAA	Lys → TERM
	1150 U → C	GUU → GCU	Val → Ala
N42-3	767 U → C	ACU → AAC	No change
N42-4	847 U → C	GUA → GCA	Val → Ala
	1002 A → G	AGU → GGU	Ser → Glu
N42-6	771 A → G	AAA → GAA	Lys → Glu
	871 U → C	GUC → GCC	Val → Ala
	1024 U → C	CUU → CCU	Leu → Pro
N42-7	740 U → C	AGU → AGC	No change
	934 A → C	CAG → CCG	Gln → Pro
	1146 G → A	GCA → ACA	Ala → Thr
N42-8	1034 G → A	UUG → UUA	No change
N42-9	949 A → U	AAG → AUG	Lys → Met
	1061 U → C	UUU → UUC	No change
N42-10	941 U → C	UGU → UGC	No change
	1049 U → C	GGU → GGC	No change
N42-11	868 A → G	GAA → AGG	Lys → Arg
N42-12	792 A → G	AUU → GUU	Ile → Val
	911 U → C	ACU → GGG	No change
	1109 A → G	GGA → GGG	No change
N42-18	912 C → U	CCA → UCA	Pro → Ser

striking examples of positive Darwinian evolution in viruses is that of Influenza A virus (Fitch *et al.*, 1991). In the case of Influenza A virus, at least two significant factors contribute to rapid evolution of the virus; the high mutation rate of the viral polymerase, and the selection of mutations which allow the virus to escape immune surveillance. Like Influenza virus, coronaviruses are replicated by a viral RNA-dependent RNA polymerase with no known proofreading activity and may evolve rapidly through random polymerase errors (Lai, 1990). In the MHV-infected animal, the immune system may play a role in neutralizing the wild-type virus and allowing viruses which have altered or deleted epitopes to propagate. The strong selection for specific S1 region deletion variants has been shown previously by isolating and characterizing attenuated variants of coronavirus (Dalziel *et al.*, 1986; Fleming *et al.*, 1986; Morris *et al.*, 1989; Parker *et al.*, 1989; La Monica *et al.*, 1991; Wang *et al.*, 1992). These attenuated variants have been shown to have significant deletions or point mutations in the spike glycoprotein gene, predominantly in the S1 "hypervariable" region (Banner *et al.*, 1990; Wang *et al.*, 1992). Our results indicate that mutations which encode amino acid changes are not limited to the S1 hypervariable region but also occur in the nucleocapsid region and potentially throughout the genome. Mutations are probably generated by errors introduced randomly throughout the genome (Steinhauer and Holland, 1987). Our results are consistent with the observations of Yokomori *et al.*, who showed that multiple HE protein-defective mutants are generated during both acute and subacute phases of viral infection in the mouse brain (Yokomori *et al.*, 1993).

The second feature of the mutations detected in the persistent coronavirus sequences is that the mutations are biased, with 63% of the mutations being U to C or A to G transitions. This type of "biased hypermutation" has been previously described in association with persistent infection of measles virus which results in measles inclusion body encephalitis (Cattaneo *et al.*, 1988). Although the mechanism for generating biased mutations is not known, it has been proposed to occur during inefficient or partially blocked stages in viral replication (Bass *et al.*, 1989). Such inefficient replication may occur if double-

TABLE 5

Summary of Mutations Detected in the Nucleocapsid Region during Persistent MHV-JHM Infection

Days postinfection	Clones sequenced	Total mutations detected	Type of mutation[a]				Mutations per thousand nucleotides sequenced
			S	C	Del	Term	
4	20	11	5	6	0	0	1.1
20	4	4	1	3	0	0	2.0
42	20	23	8	14	0	1	2.4

[a] S, silent; C, change of amino acid; Del, deletion; Term, termination codon.

TABLE 6

Type of Nucleotide Change Occurring in the S and N RNA during Persistent Infection

	Transition				Transversion							
	U → C	C → U	G → A	A → G	U → A	A → U	G → C	C → G	U → G	G → U	A → C	C → A
S — Day 4	8	2	4	6	0	0	2	0	0	0	0	0
S — Day 8	1	0	2	1	0	0	0	0	0	0	0	0
S — Day 13	4	0	3	1	0	1	0	0	0	1	0	0
S — Day 20	4	0	1	2	0	0	0	0	0	0	0	0
S — Day 42	17	6	6	15	3	3	0	1	2	0	0	1
S — Total	34	8	16	25	3	4	2	1	2	1	0	1
N — Day 4	3	2	1	3	0	1	0	0	0	0	1	0
N — Day 20	1	0	0	2	1	0	0	0	0	0	0	0
N — Day 42	11	1	2	6	0	2	0	0	0	0	1	0
N — Total	15	3	3	11	1	3	0	0	0	0	2	0

stranded RNAs (dsRNA) are stable intermediates of replication. For replication to occur from a dsRNA, a putative viral or cellular helicase activity is required to unwind the RNA. Such a dsRNA unwinding/modifying activity has been characterized in human cells (Bass and Weintraub, 1988). This enzyme can modify adenosine residues to inosine residues, resulting in a destabilizing of the double-stranded RNA and unwinding, thereby allowing elongation by the RNA polymerase (Wagner *et al.*, 1989). The result of the modification of adenosine to inosine is a predominance of A to G and U to C mutations during the replication of plus- and minus-strand RNA (Bass *et al.*, 1989). Clearly, biased hypermutations are much more prevalent in measles virus persistent infection as compared to coronavirus persistent infection (there are greater than 50% U to C transitions and over 20% of the U residues in certain regions are changed to C in persistent measles RNA, Wong *et al.*, 1991). However, it is interesting to speculate that a similar mechanism for generating biased mutations may contribute to the mutations seen in two different types of viral persistent CNS infections, measles and coronavirus.

The mechanism by which the mutant viral RNAs are generated and the importance of selective pressures (immune system, neuron or glial cell environment, and viral replication competency) exerted on the persistent viral RNA remains to be determined. The mutations may be introduced randomly by the viral RNA-dependent RNA polymerase during replication. Error rates for viral RNA polymerases have been estimated to be on the order of 10^{-4} to 10^{-5} (Steinhauer and Holland, 1987; Parvin *et al.*, 1986; De La Torre *et al.*, 1992). The high error rate during replication allows for rapid evolution (Steinhauer and Holland, 1987; Holland *et al.*, 1982). Mutations may also be introduced by the dsRNA unwinding/modifying activity as described above (Bass *et al.*, 1989; Wong *et al.*, 1991; Rataul *et al.*, 1992). The mutant or defective viral genomes generated during this process may have an advantage in the persistently infected cell by being unable to synthesize infectious virus and therefore escaping immune recognition. The diverse population or "quasispecies" (Eigen, 1993) of RNAs that we detect in coronavirus persistent infection may reflect the multiple pathways that are used to generate and maintain the persistent viral RNA.

The role of persistent coronavirus RNA in the pathogenesis of chronic demyelination remains to be elucidated. The persistent viral RNA may be translated at low levels, resulting in chronic antigenic stimulation at sites of viral infection. Alternatively, persistent viral RNA sequences could result in abnormal neuronal or glial cell function, potentially disrupting normal CNS functions. Reactivation of latent or defective virus may be another mechanism contributing to pathogenesis in persistent coronavirus infection. Studies with the Sindbis virus (SV) model system for acute encephalitis infection of mice have demonstrated that SV RNA persists in neurons of infected mice for at least 17 months after infection (Levine and Griffin, 1992). Interestingly, the persistent Sindbis virus can be reactivated under conditions of waning antibody titer (Levine and Griffin, 1992). Further study of coronavirus persistence in the absence of immune selection *in vivo* (in SCID mice) may shed light on the mechanisms involved in the generation of mutant viruses and the role of persistent viral RNA in the pathogenesis of chronic demyelination.

ACKNOWLEDGMENTS

We thank Colette Ruedin for excellent technical assistance. This work was supported by Public Health Service Research Grant AI32065 from the National Institutes of Health, a Junior Faculty Research Award from the American Cancer Society (to S.C.B.), and National Multiple Sclerosis Society Research Grant RG2283-A-2 (to J.O.F.).

REFERENCES

Baczko, K., Liebert, U. G., Billeter, M. A., Cattaneo, R., Budka, H., and ter Meulen, V. (1986). Expression of defective measles virus genes in brain tissues of patients with subacute sclerosing panencephalitis. *J. Virol.* **59,** 472–478.

Banner, L. R., Keck, G. K., and Lai, M. M. C. (1990). A clustering of RNA recombination sites adjacent to a hypervariable region of the peplomer gene of murine coronavirus. *Virology* **175,** 548–555.

Bass, B. L., and Weintraub, H. (1988). An unwinding activity that covalently modifies its double-stranded RNA substrate. *Cell* **55,** 1089–1098.

Bass, B. L., Weintraub, H., Cattaneo, R., and Billeter, M. A. (1989). Biased hypermutation of viral RNA genomes could be due to unwinding/modification of double-stranded RNA. *Cell* **56,** 331.

Cattaneo, R., Schmid, A., Eschle, D., Baczko, K., ter Meulen, V., and Billeter, M. (1988). Biased hypermutations and other genetic changes in defective measles viruses in human brain infection. *Cell* **55,** 255–265.

Chang, S. Y., Shih, A., and Kwok, S. (1993). Detection of variability in natural populations of viruses by polymerase chain reaction. *In* "Methods in Enzymology" (E. A. Zimmer, T. J. White, R. L. Cann, and A. C. Wilson, Eds.), Vol. 224, pp. 428–432. Academic Press, San Diego.

Chao, Y.-C., Chang, M.-F., Gust, I., and Lai, M. M. C. (1990). Sequence conservation and divergence of hepatitis delta virus RNA. *Virology* **178,** 384–392.

Choo, Q.-L., Richman, K. H., Han, J. H., Berger, K., Lee, C., Dong, C., Gallegos, C., Coit, D., Medina-Selby, A., Barr, P. J., Weiner, A. J., Bradley, D. W., Kuo, G., and Houghton, M. (1991). Genetic organization and diversity of the hepatitis C virus. *Proc. Natl. Acad. Sci. USA* **88,** 2451–2455.

Dalziel, R. G., Lampert, P. W., Talbot, P. J., and Buchmeier, M. J. (1986). Site specific alteration of murine hepatitis virus type 4 peplomer glycoprotein E2 results in reduced neurovirulence. *J. Virol.* **59,** 463–471.

De La Torre, J. C., Giacchetti, C., Semler, B. L., and Holland, J. J. (1992). High frequency of single-base transitions and extreme frequency of precise multiple-base reversion mutations in poliovirus. *Proc. Natl. Acad. Sci. USA* **89,** 2531–2535.

Eigen, M. (1993). The origin of genetic information: Viruses as models. *Gene* **135,** 37–47.

Fitch, W. M., Leiter, J. M. E., Li, X., and Palese, P. (1991). Positive Darwinian evolution in human influenza A viruses. *Proc. Natl. Acad. Sci. USA* **88,** 4270–4274.

Fleming, J. O., Trousdale, M. D., El-Zaatari, F. A. K., Stohlman, S., and Weiner, L. P. (1986). Pathogenicity of antigenic variant of murine coronavirus JHM selected with monoclonal antibodies. *J. Virol.* **58,** 869–875.

Fleming, J. O., and Pen, L. B. (1988). Measurement of the concentration of murine IgG monoclonal antibody in hybridoma supernatants and ascites in absolute units by sensitive and reliable enzyme-linked immunosorbent assay (ELISA). *J. Immunol. Methods* **110,** 8–11.

Higashi, Y., Kakumu, S., Yoshioka, K., Wakita, T., Mizokami, M., Ohba, K., Ito, Y., Ishikawa, T., Takayanagi, M., and Naga, Y. (1993). Dynamics of genome change in the E2/NS1 region of hepatitis C virus *in vivo*. *Virology* **197,** 659–668.

Holland, J., Spindler, K., Horodyski, F., Grabau, E., Nichol, S., and Vande-Pol, S. (1982). Rapid evolution of RNA genomes. *Science* **215,** 1577–1585.

Knobler, R. L., Lampert, P. W., and Oldstone, M. B. A. (1982). Virus persistence and recurring demyelination produced by a temperature-sensitive mutant of MHV-4. *Nature* **298,** 279–280.

Kyuwa, S., and Stohlman, S. (1990). Pathogenesis of a neurotropic murine coronavirus, strain JHM in the central nervous system of mice. *Semin. Virol.* **1,** 273–280.

Lai, M. M. C. (1990). Coronavirus: Organization, replication and expression of genome. *Annu. Rev. Microbiol.* **44,** 303–333.

La Monica, N., Banner, L. R., Morris, V. L., and Lai, M. M. C. (1991). Localization of extensive deletions in the structural genes of two neurotropic variants of murine coronavirus JHM. *Virology* **182,** 883–888.

Lee, C.-M., Bih, F.-Y., Chao, Y. C., Govindarajan, S., and Lai, M. M. C. (1992). Evolution of hepatitis delta virus RNA during chronic infection. *Virology* **188,** 265–273.

Levine, B., and Griffin, D. (1992). Persistence of viral RNA in mouse brains after recovery from acute alphavirus encephalitis. *J. Virol.* **66,** 6429–6435.

Martell, M., Esteban, J. I., Quer, J., Genesca, J., Weiner, A., Esteban, R., Guardia, J., and Gomez, J. (1992). Hepatitis C virus (HCV) circulates as a population of different but closely related genomes: Quasispecies nature of HCV genome distribution. *J. Virol.* **66,** 3225–3229.

Morris, V. L., Tieszer, C., Mackinnon, J., and Percy, D. (1989). Characterization of coronavirus JHM variants isolated from Wistar Furth rats with a viral-induced demyelinating disease. *Virology* **169,** 127–136.

Oldstone, M. B. A. (1989). Viral persistence. *Cell* **56,** 517–520.

Oldstone, M. B. A. (1991). Molecular anatomy of viral persistence. *J. Virol.* **65,** 6381–6386.

Parker, S. E., Gallagher, T. M., and Buchmeier, M. J. (1989). Sequence analysis reveals extensive polymorphism and evidence of deletions within the E2 peplomer glycoprotein coding regions of several strains of murine hepatitis virus. *Virology* **173,** 664–673.

Parvin, J. D., Moscona, A., Pan, W. T., Leider, J. M., and Palese, P. (1986). Measurement of the mutation rates of animal viruses: Influenza A virus and poliovirus type 1. *J. Virol.* **59,** 377–383.

Rataul, S. M., Hirano, A., and Wong, T. C. (1992). Irreversible modification of measles virus RNA in vitro by nuclear RNA-unwinding activity in human neuroblastoma cells. *J. Virol.* **66,** 1769–1773.

Saiki, R. K., Gelfand, D. H., Stoffel, S., Scharf, S. J., Higuchi, R., Horn, G. T., Mullis, K. B., and Erlich, H. A. (1988). Primer-directed enzymatic amplification of DNA with a thermostable DNA polymerase. *Science* **239,** 487–491.

Sanger, F., Nicklen, S., and Coulson, A. R. (1977). DNA sequencing with chain-terminating inhibitors. *Proc. Natl. Acad. Sci. USA* **74,** 5463–5467.

Spaan, W., Cavanagh, D., and Horzinek, M. C. (1990). *In* "Immunochemistry of Viruses. II. The Basis for Serodiagnosis and Vaccines" (M. H. V. van Regenmortel and A. R. Neurath, Eds.), pp. 359–379. Elsevier, New York.

Steinhauer, D. A., and Holland, J. J. (1987). Rapid evolution of RNA viruses. *Annu. Rev. Microbiol.* **41,** 409–433.

Wagner, R. W., Smith, J. E., Cooperman, B. S., and Nishikuro, K. (1989). A double stranded RNA unwinding activity introduces structural alterations by means of adenosine to inosine conversions in mammalian cells and Xenopus eggs. *Proc. Natl. Acad. Sci. USA* **86,** 2647–2651.

Wang, F.-I., Fleming, J. O., and Lai, M. M. C. (1992). Sequence analysis of the spike protein gene of murine coronavirus variants: Study of genetics sites affecting neuropathogenicity. *Virology* **186,** 742–749.

Wong, T. C., Ayata, M., Ueda, S., and Hirano, A. (1991). Role of biased hypermutation on evolution of subacute sclerosing panencephalitis virus from progenitor acute measles virus. *J. Virol.* **65,** 2191–2199.

Yokomori, K., Stohlman, S. A., and Lai, M. M. C. (1993). The detection and characterization of multiple hemagglutinin-esterase (HE)-defective viruses in the mouse brain during subacute demyelination induced by mouse hepatitis virus. *Virology* **192,** 170–178.